
Addressing the Scarcity of Benchmarks for Graph XAI

Michele Fontanesi, Alessio Micheli, Marco Podda, Domenico Tortorella

Department of Computer Science

University of Pisa

Largo B. Pontecorvo, 3, Pisa, Italy 56127

michele.fontanesi@phd.unipi.it,

{alessio.micheli,marco.podda,domenico.tortorella}@unipi.it

Abstract

While Graph Neural Networks (GNNs) have become the *de facto* model for learning from structured data, their decisional process remains opaque to the end user, undermining their deployment in safety-critical applications. In the case of graph classification, Explainable Artificial Intelligence (XAI) techniques address this major issue by identifying sub-graph motifs that explain predictions. However, advancements in this field are hindered by a chronic scarcity of benchmark datasets with known ground-truth motifs to assess the explanations' quality. Current graph XAI benchmarks are limited to synthetic data or a handful of real-world tasks hand-curated by domain experts. In this paper, we propose a general method to automate the construction of XAI benchmarks for graph classification from real-world datasets. We provide both 15 ready-made benchmarks, as well as the code to generate more than 2000 additional XAI benchmarks with our method. As a use case, we employ our benchmarks to assess the effectiveness of some popular graph explainers.

1 Introduction

Graphs are data structures that allow a flexible representation of entities and their relationships as nodes and edges, respectively. Currently, the leading technology for learning from graph data is Graph Neural Networks (GNNs) (Bacciu et al., 2020). Since their inception in convolutional (Micheli, 2009) or recursive (Scarselli et al., 2009) form, GNNs have shown promising results in a variety of applications. The strength of GNNs lies in their ability of learning graph representations adaptively from data without needing feature engineering. However, as their adoption becomes widespread, so does the necessity of making their predictive mechanisms transparent to stakeholders and end-users, allowing informed decision-making in alignment with current legal and ethical standards, such as the European Union's General Data Protection Regulation (GDPR) (Goodman and Flaxman, 2016), and to support the scientific discovery process (Alizadehsani et al., 2024).

To contribute to this objective, different eXplainable Artificial Intelligence (XAI) techniques for graph data, also known as *graph explainers*, have been developed (Yuan et al., 2023; Kakkad et al., 2023) to elucidate GNN predictions. In graph classification tasks, where GNNs learn to map entire graphs to discrete classes, an explanation corresponds to one or more subgraphs that drive the GNN prediction towards the correct class. Therefore, graph explainers try to identify explanations by assigning real-valued importance scores to the graph components (typically nodes, but also edges or features), which can be thresholded to recover possible explanatory substructures. To assess their effectiveness, graph explainers are evaluated according to the following pipeline, which includes:

1. selecting (or generating) benchmark datasets that include ground-truth (GT) explanations;
2. training a GNN to high test accuracy on the datasets;

3. passing the trained GNN and a test set of graphs *post-hoc* to the graph explainer to obtain a set of importance scores for each graph;
4. quantifying how well the subgraphs produced by the explainer overlap with the assumed GTs with appropriate metrics.

Among these steps, selecting or generating benchmark datasets with reliable GT explanations is especially critical: without robust benchmarks, comparisons become misleading, ultimately causing scientists to misdirect their research efforts. As widely known, the abundance of high-quality benchmark datasets has arguably been one of the key factors to drive progress in fields like computer vision (Deng et al., 2009) and natural language processing (Wang et al., 2018). Most graph XAI benchmarks rely on generated datasets, which offer a controlled and reproducible environment to evaluate explainers. Samples in these datasets are constructed by attaching artificial GT motifs (e.g. grid graphs or house graphs) to randomly sampled graphs, typically using preferential attachment. Although these datasets are easy to generate and widely supported by most graph XAI benchmarks, they all crucially lack the structural complexity and variability of real-world graphs. Conversely, only few datasets are based on real-world graphs (Sanchez-Lengeling et al., 2020; Varbella et al., 2024; Agarwal et al., 2023), mainly due to the necessary domain expertise required to annotate the GT explanations. We find the current situation of graph XAI benchmarking unfit for continuous progress. On the one hand, generated datasets are numerous but hardly challenging for graph explainers, leading to overestimating their true capabilities and preventing their improvement. On the other hand, the scarcity of graph XAI datasets based on realistic graphs makes any “field-test” comparison among graph explainers severely biased by statistical fluctuations, making it hard to understand which direction for improvement is worth researching.

To close this gap and support the systematic development of novel XAI methods for graph-structured data, we propose a method to automatically generate binary graph classification datasets with integrated GT explanations from existing real-world datasets. Specifically, we apply the Weisfeiler-Leman coloring algorithm (Weisfeiler and Leman, 1968) to existing graph classification datasets, and use the resulting coloring to identify subsets of graphs sharing identical substructures in each of the classes. Then, we extract subsets of the original task for which a substructure acts as a discriminating pattern for the classification target label, and we treat their shared common substructure as the GT explanation for that target. Notably, while the resulting benchmark dataset is essentially a synthetic restriction of the original task, the GT explanations are actual structural patterns of the originating graph, in stark contrast with artificially generated datasets. We employ this methodology to build the initial core of the OPENGRAPHXAI benchmark, a collection of 15 novel graph-XAI datasets derived from 11 existing molecular graph datasets. The collection is easily extensible to 2000+ datasets, and we provide the code and tools to support any extension. We demonstrate the utility of the OPENGRAPHXAI benchmark by evaluating several prominent graph explainers from the literature, showing that this collection is not only useful for rigorous benchmarking but also instrumental to reason about the capabilities and limitations of current graph XAI methods.

We anticipate that this contribution will play a role in advancing progress and shaping research priorities in the field of graph XAI, and, consequently, enhancing the trustworthiness of graph machine learning methodologies (Oneto et al., 2022).

2 Related works

The assessment of graph explainers (Yuan et al., 2023; Kakkad et al., 2023) relies on evaluating the quality of the explanations they yield. Since the inception of the first explainers for GNNs (Baldassarre and Azizpour, 2019; Pope et al., 2019; Ying et al., 2019; Luo et al., 2020), the development of appropriate metrics and benchmarks has been a key focus in the field. Metrics to evaluate graph explainers include unsupervised ones such as fidelity (Pope et al., 2019; Amara et al., 2022; Longa et al., 2025), which quantifies the degree to which the explanation reflects the GNN’s output, or supervised ones like plausibility (Rathee et al., 2022), which measures how well the explanation aligns with the GT explanation associated with a given class. Other metrics cover additional desiderata such as sparseness (succinctness) and connectedness (compactness) of the explanations.

Benchmark datasets with integrated GTs for the evaluation of graph explainers have predominantly been of synthetic nature, typically by augmenting randomly generated Barabási-Albert (BA) graphs with explanatory motifs. For example, in the BA2Grid dataset (Luo et al., 2020), positive samples are

BA graphs with a grid graph motif attached, while negative samples are random BA graphs without an attached motif. Among other synthetic datasets, we mention BA2Motif, GridHouse, HouseColors, and Stars (Longa et al., 2025). However, these datasets suffer from key limitations (Faber et al., 2021). For example, Fontanesi et al. (2024) discovered that despite being trained to perfect accuracy, different GNN architectures rely on different, but equally valid, explanations than the original GTs.

Real-world graph XAI datasets have been introduced by Sanchez-Lengeling et al. (2020) and later included and extended in the GraphXAI library (Agarwal et al., 2023). These datasets are based on chemical molecules from known data sources (Riesen and Bunke, 2008; Kazius et al., 2005; Sterling and Irwin, 2015), and are designed for binary graph classification tasks. They include a variant of Mutagenicity (Kazius et al., 2005), and three subsets of the Zinc15 database (Sterling and Irwin, 2015), namely FluorideCarbonyl, AlkaneCarbonyl, and Benzene. Their GT explanations have been established by leveraging chemical domain expertise. Specifically, the Mutagenicity dataset distinguishes molecules based on the presence of known toxicophores such as NH_2 , NO_2 , aliphatic halide, nitroso, and azo-type. The FluorideCarbonyl and AlkaneCarbonyl datasets classify molecules based on the co-occurrence of a fluoride and carbonyl or an alkane and carbonyl functional group, respectively. Lastly, the Benzene dataset distinguishes molecules containing at least one benzene ring from those that lack one. In contrast, the dataset proposed by Varbella et al. (2024) features GT explanations for cascading failure analysis in power grids, which have been derived through computer model simulations. In general, datasets with GT explanations based on real-world graphs are difficult to generate, as identifying the GT motifs associated with the classes requires the knowledge and effort of a domain expert. This complexity explains their limited availability in the literature.

All the datasets mentioned above are routinely collected into benchmarks by common graph XAI libraries (Agarwal et al., 2023; Amara et al., 2022; Rathee et al., 2022; Varbella et al., 2024). Our approach to overcoming the limitations of current practices for dataset collation in graph XAI is orthogonal and leverages an algorithm to extract synthetic explanatory subgraphs from curated subsets of real-world datasets. Therefore, our approach has the distinctive advantage that GT explanations are derived from the same structural patterns as the originating graph datasets.

3 Constructing XAI benchmarks for graph classification

To be suitable for XAI, a graph classification dataset must be augmented with an explanation for the class assignment of each of its samples. Such an explanation takes the form of one or more motifs, i.e. sub-graph patterns, whose presence or absence is sufficient to discriminate the graph’s class. In this section, we describe a method to automate this benchmark construction pipeline, based on two steps:

1. First, mine a large set of potential sub-graph motifs of different sizes, balancing exhaustiveness and computational cost.
2. Then, generate a collection of suitable XAI benchmarks from the set of potentially discriminating motifs.

Our method can be applied to any graph classification dataset with discrete input features, making it particularly suitable in the case of chemical data.

3.1 Weisfeiler–Leman coloring and sub-graph patterns

Let $\mathcal{G}(\mathcal{V}, \mathcal{E})$ be a graph, with \mathcal{V} its set of nodes and \mathcal{E} its edges; the set of neighbors of v is denoted by \mathcal{N}_v . Each node $v \in \mathcal{V}$ may have an input label $x_v \in \mathcal{X}$, where \mathcal{X} is a finite set, e.g. the set of atom types in a molecule. We also define $d_{\mathcal{G}}(v, u)$ as the shortest-path distance from v to u , and $\text{Ego}_{\mathcal{G}}^L(v) = \{u \in \mathcal{V} : d_{\mathcal{G}}(v, u) \leq L\}$ as the set of nodes that belong to the L -radius ego-graph of v .

A motif \mathbf{m} is a connected sub-graph $\mathcal{G}' \sqsubset \mathcal{G}$, i.e. a connected graph $\mathcal{G}'(\mathcal{V}', \mathcal{E}')$ such that $\mathcal{V}' \subset \mathcal{V}$, $\mathcal{E}' \subset \mathcal{E}'$ and $x'_v = x_v$ for all $v \in \mathcal{V}'$. Systematically mining sub-graph motifs can be a costly operation (Xifeng Yan and Jiawei Han, 2002; Yan et al., 2008; Elseid et al., 2014; Packer and Holder, 2017), due also to the sub-graph isomorphism problem being NP-complete (Ullmann, 1976). We therefore resort to the Weisfeiler–Leman (WL) node coloring algorithm (Weisfeiler and Leman, 1968; Morris et al., 2023), that has been employed as a heuristic test of graph isomorphism thanks to its computational complexity of $O(|\mathcal{E}| \log |\mathcal{V}|)$.

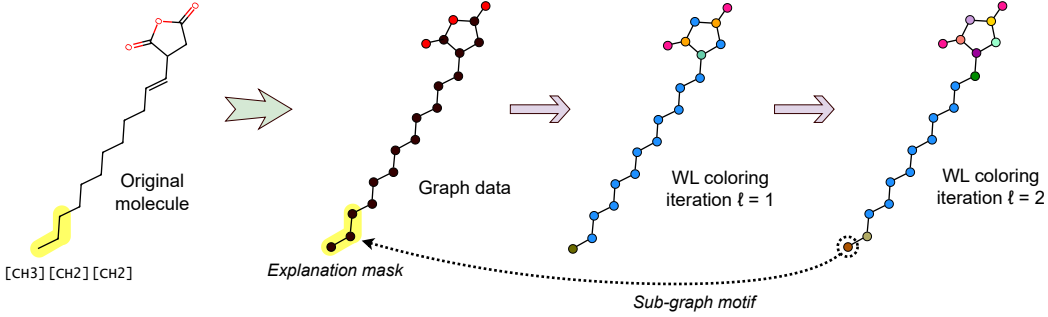


Figure 2: In a chemical dataset, molecules are transformed into graphs. WL coloring is used to mine the set of sub-graph motifs available for the construction of our XAI benchmarks. A motif corresponding to the WL label $m \in \mathcal{C}_2$ has been chosen. The explanation mask is constituted by the 2-radius ego-graphs of nodes with WL color m . In this example, the motif can be traced back to the fragment $[\text{CH3}] [\text{CH2}] [\text{CH2}]$.

Starting from an initial set of colors $\mathcal{C}_0 = \mathcal{X}$ and node ‘colors’ (or labels) $h_v^{(0)} = x_v$, each WL iteration $\ell > 0$ assigns a new node color $h_v^{(\ell)} \in \mathcal{C}_\ell$ for each unique multi-set of neighbors’ labels (as in Figure 1),

$$h_v^{(\ell)} = \text{HASH} \left(\{ \{ h_u^{(\ell-1)} : u \in \mathcal{N}_v \} \} \right). \quad (1)$$

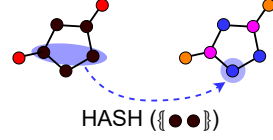


Figure 1: WL coloring.

If two nodes v, u have equal labels $h_v^{(\ell)} = h_u^{(\ell)}$, then their unfolding trees of depth ℓ are equal (Kriege, 2022; D’Inverno et al., 2024). This means that each color in \mathcal{C}_ℓ identifies ego sub-graphs of radius ℓ that belong to the same congruence class in the ℓ -th WL iteration. After L iterations, the graph \mathcal{G} is represented by its WL histogram $H_{\mathcal{G}} = \bigcup_{\ell=0}^L \{ \{ h_v^{(\ell)} : v \in \mathcal{V} \} \}$. The color set $\mathcal{C} = \bigcup_{\ell=0}^L \mathcal{C}_\ell$ represents a set of sub-graph motifs $m \in \mathcal{C}$ whose presence in \mathcal{G} can be easily checked by testing if $m \in H_{\mathcal{G}}$.

Interestingly, WL isomorphism constitutes the theoretical upper-bound of expressiveness in GNNs (Xu et al., 2019). In particular, a GNN with L message-passing layers cannot distinguish more graphs than an L -iterations WL test (D’Inverno et al., 2024). Therefore, we are assured that sub-graph motifs $m \in \mathcal{C}$ can potentially be discovered by the learning models that XAI methods aim to explain.

3.2 Automating the construction of XAI benchmarks

A XAI benchmark dataset for binary graph classification is a collection of triplets $(\mathcal{G}, y_{\mathcal{G}}, \mathcal{M}_{\mathcal{G}})$, where \mathcal{G} is the graph sample, $y_{\mathcal{G}} \in \{0, 1\}$ is its class, and $\mathcal{M}_{\mathcal{G}} \subset \mathcal{V}$ is the GT mask, i.e. the sub-set of nodes that belong to a motif m explaining the class assignment.

XAI benchmarks can have:

- either an explanation motif m_y for each of the classes, i.e. $y_{\mathcal{G}} = 0 \iff m_0 \sqsubset \mathcal{G} \wedge m_1 \not\sqsubset \mathcal{G}$ and $y_{\mathcal{G}} = 1 \iff m_1 \sqsubset \mathcal{G} \wedge m_0 \not\sqsubset \mathcal{G}$,
- or a single explanation motif m whose presence or absence discriminates between classes, e.g. $y_{\mathcal{G}} = 0 \iff m \sqsubset \mathcal{G}$ and $y_{\mathcal{G}} = 1 \iff m \not\sqsubset \mathcal{G}$.

To generate a XAI benchmark from a binary graph classification task $\mathcal{D} = \{(\mathcal{G}, y_{\mathcal{G}})\}$, we must find a subset of graph samples $\mathcal{D}' \subseteq \mathcal{D}$ and a motif m (respectively a pair of motifs m_0, m_1) that can discriminate the class assignment in \mathcal{D}' .

We side-step the sub-graph isomorphism problem by working with WL histograms $H_{\mathcal{G}}$ instead of graphs, and WL labels $m \in \mathcal{C}$ instead of sub-graph motifs. Once a discriminating WL label $m \in \mathcal{C}_\ell$ has been chosen, the explanation mask for graph \mathcal{G} is constituted of the ego graphs of m -colored nodes, that is $\mathcal{M}_{\mathcal{G}} = \bigcup_{v \in \mathcal{V}, h_v^{(\ell)} = m} \text{Ego}_{\mathcal{G}}^\ell(v)$. This process is illustrated in Figure 2.

Since considering all possible WL colors and color pairs is still computationally onerous, we propose a heuristic approach based on the frequencies of WL labels in the respective classes. Let $\text{freq}_y(\mathbf{m}) = \sum_{\mathcal{G} \in \mathcal{D}} \mathbf{1}[\mathbf{m} \in \mathbf{H}_{\mathcal{G}} \wedge y_{\mathcal{G}} = y]$ be the number of graphs of class y where $\mathbf{m} \in \mathcal{C}$ occurs, and let $\Delta\text{freq}(\mathbf{m}) = \text{freq}_1(\mathbf{m}) - \text{freq}_0(\mathbf{m})$. The best candidate as discriminating WL labels for class 1 (resp. class 0) would be the \mathbf{m} 's with largest (resp. smallest) $\Delta\text{freq}(\mathbf{m})$, as they are the most skewed towards one of the classes. Once the candidate labels have been selected, the XAI benchmark $\mathcal{D}_{\text{XAI}} = \{(\mathcal{G}, y_{\mathcal{G}}, \mathcal{M}_{\mathcal{G}})\}$ is generated by collecting graphs that satisfy the label-class assignment, along with the GT masks obtained via the ego sub-graphs. The procedure is detailed in Algorithm 1.

Algorithm 1 Generate graph XAI datasets from real-world graph datasets

Require: Binary graph classification dataset \mathcal{D} , number of WL iterations $L > 0$, maximum number of candidate WL labels $K > 0$

- 1: Compute WL histograms $\mathbf{H}_{\mathcal{G}}$ with L iterations for all $\mathcal{G} \in \mathcal{D}$
- 2: Compute class frequencies $\text{freq}_y(\mathbf{m})$ for all WL labels $\mathbf{m} \in \mathcal{C}$
- 3: $\hat{\mathcal{C}}_1 \leftarrow \{\mathbf{m} \in \mathcal{C} : \mathbf{m} \in \text{TOP}_K(\Delta\text{freq}(\mathbf{m}))\}$, $\hat{\mathcal{C}}_0 \leftarrow \{\mathbf{m} \in \mathcal{C} : \mathbf{m} \in \text{TOP}_K(-\Delta\text{freq}(\mathbf{m}))\}$
- 4: **for** $\mathbf{m}_0, \mathbf{m}_1 \in \hat{\mathcal{C}}_0 \times \hat{\mathcal{C}}_1$ **do** ▷ generate benchmarks with explanations for both classes
- 5: $\mathcal{D}_0 \leftarrow \left\{ \left(\mathcal{G}, 0, \bigcup_{v \in \mathcal{V}, \mathbf{h}_v^{(\ell)} = \mathbf{m}_0} \text{Ego}_{\mathcal{G}}^{\ell}(v) \right) : \mathcal{G} \in \mathcal{D} \wedge y_{\mathcal{G}} = 0 \wedge \mathbf{m}_0 \in \mathbf{H}_{\mathcal{G}} \wedge \mathbf{m}_1 \notin \mathbf{H}_{\mathcal{G}} \right\}$
- 6: $\mathcal{D}_1 \leftarrow \left\{ \left(\mathcal{G}, 1, \bigcup_{v \in \mathcal{V}, \mathbf{h}_v^{(\ell)} = \mathbf{m}_1} \text{Ego}_{\mathcal{G}}^{\ell}(v) \right) : \mathcal{G} \in \mathcal{D} \wedge y_{\mathcal{G}} = 1 \wedge \mathbf{m}_0 \notin \mathbf{H}_{\mathcal{G}} \wedge \mathbf{m}_1 \in \mathbf{H}_{\mathcal{G}} \right\}$
- 7: **yield** $\mathcal{D}_{\text{XAI}} = \mathcal{D}_0 \cup \mathcal{D}_1$
- 8: **end for**
- 9: **for** $y \in \{0, 1\}$ **do** ▷ generate benchmarks with explanations for a single class
- 10: **for** $\mathbf{m} \in \hat{\mathcal{C}}_y$ **do**
- 11: $\mathcal{D}_y \leftarrow \left\{ \left(\mathcal{G}, y, \bigcup_{v \in \mathcal{V}, \mathbf{h}_v^{(\ell)} = \mathbf{m}} \text{Ego}_{\mathcal{G}}^{\ell}(v) \right) : \mathcal{G} \in \mathcal{D} \wedge y_{\mathcal{G}} = y \wedge \mathbf{m} \in \mathbf{H}_{\mathcal{G}} \right\}$
- 12: $\mathcal{D}_{(1-y)} \leftarrow \{(\mathcal{G}, (1-y), \emptyset) : \mathcal{G} \in \mathcal{D} \wedge y_{\mathcal{G}} = (1-y) \wedge \mathbf{m} \notin \mathbf{H}_{\mathcal{G}}\}$
- 13: **yield** $\mathcal{D}_{\text{XAI}} = \mathcal{D}_y \cup \mathcal{D}_{(1-y)}$
- 14: **end for**
- 15: **end for**

3.3 The OPENGRAPHXAI benchmark suite

We apply our method to create OPENGRAPHXAI, a curated collection of 15 novel XAI benchmarks for graph classification, listed in Table 1. All the datasets of our benchmarking suite are based on real-world molecular graphs derived from the TUDataset collection by Morris et al. (2020). They have been constructed to cover multiple GT-availability scenarios while offering mostly class-balanced tasks to solve. As part of the collection, we provide tasks featuring GT explanations for both classes of equal-size sub-graph motifs (`alfa`, `delta`) or of different sizes (`bravo`, `charlie`, `echo`), as well as datasets providing GT explanations for only one of the two classes (`foxtrot` to `oscar`). GT masks are illustrated in Appendix A. We also provide suggested scaffold splits into 70% training, 20% validation, and 10% test sets for each benchmark, with samples stratified by class and graph size. As supplementary material, we make available the WL labels to generate an extended collection of 2000+ benchmarks from other TU datasets.

4 Evaluating graph explainers: A use case

To showcase the contribution that a large collection of benchmarks such as ours can make to the research in graph XAI, we perform an experimental evaluation of a set of explainer methods for graph classification. Specifically, we focus on *post-hoc* local explainers on a trained GNN model that achieves a high performance on the classification tasks, and measure how well the explanations align with the GT masks in each of the OPENGRAPHXAI benchmarks.

4.1 Setting

Model to explain A GNN is a deep neural network model that addresses a graph classification task by learning a hierarchy of node representations $\mathbf{h}_v^{(\ell)} \in \mathbb{R}^{d'}$ in each of its layers. New representations

Table 1: Datasets in the OPENGRAPHXAI benchmark suite. The Balance column reports the ratio between the minority class and the majority class.

Task	Original dataset	WL label iterations		Samples			Balance
		class 0	class 1	class 0	class 1	total	
alfa	NCI1	3	3	505	598	1103	0.84
bravo	NCI1	3	1	573	551	1124	0.96
charlie	NCI1	0	3	463	543	1006	0.85
delta	NCI109	3	3	515	563	1078	0.91
echo	NCI109	3	2	598	558	1156	0.93
foxtrot	NCI109	—	2	1195	987	2182	0.83
golf	TOX21_AHR	4	—	833	962	1795	0.87
hotel	TOX21_ER-LBD	4	—	444	457	901	0.97
india	TOX21_P53	4	—	658	590	1248	0.90
juliett	TOX21_ER-LBD	5	—	563	455	1018	0.81
kilo	MCF-7	3	—	2007	1978	3985	0.99
lima	MOLT-4	3	—	3086	2786	5872	0.90
mike	P388	3	—	2444	2225	4669	0.91
november	PC-3	2	—	1609	1531	3140	0.95
oscar	SW-620	3	—	2340	2273	4613	0.97

$\mathbf{h}_v^{(\ell)}$ are computed from the previous ones via graph convolution or message-passing, an operation akin to the WL coloring of Eq. (1),

$$\mathbf{h}_v^{(\ell)} = \text{AGGREGATE} \left(\left\{ \text{MESSAGE}(\mathbf{h}_v^{(\ell-1)}, \mathbf{h}_u^{(\ell-1)}) : u \in \mathcal{N}_v \right\} \right). \quad (2)$$

The global graph representation $\mathbf{H}_{\mathcal{G}} = \text{AGGREGATE}(\{\mathbf{h}_v^{(\ell-1)} : v \in \mathcal{V}\})$ is fed to a readout classifier $\hat{y}_{\mathcal{G}} = F_{\theta}(\mathbf{H}_{\mathcal{G}})$. The resulting architecture is trained end-to-end by optimizing the binary cross-entropy loss function. As the particular GNN model for our experiments, we adopt Graph Isomorphism Networks (GIN), a widely used GNN for graph classification tasks that can theoretically achieve the upper bound of expressiveness of the WL isomorphism test (Xu et al., 2019). Details on the hyper-parameter selection and the training of GIN for our experiments are reported in Appendix B.

Explainers Local *post-hoc* explainers for GNNs are method that compute a mask $\hat{\mathbf{m}}_{\mathcal{G}} \in \mathbb{R}^{|\mathcal{V}|}$ that assigns importance scores to the nodes of \mathcal{G} based on their relevance to the model prediction. Along with the **Random** baseline that assigns random importance values to nodes, in our experiments we consider four other examples of graph explainers. From the class of gradient-based methods, we consider **Saliency**, which was initially applied to the image domain (Simonyan et al., 2014) and then adapted for GNNs (Baldassarre and Azizpour, 2019; Agarwal et al., 2023), and **Integrated Gradients** (IG) (Sundararajan et al., 2017). **GNNEExplainer** (GNNEExpl) (Ying et al., 2019) is one of the most widely adopted explainable AI techniques for GNNs, and it is based on mutual information maximization. Finally, **Class Activation Mapping** (CAM) (Zhou et al., 2016; Pope et al., 2019) is a model-specific technique that quantifies the contribution of each node to the logits of the global readout classifier. A detailed description of these methods can be found in Appendix D.2.

Evaluation metric To measure the alignment between an explanation $\hat{\mathbf{m}}_{\mathcal{G}}$ and a GT mask $\mathcal{M}_{\mathcal{G}}$ we adopt the *plausibility* metric (Rathee et al., 2022; Longa et al., 2025), which is defined as the area under the ROC curve (AUC) of the importance mask with respect to the GT mask. We report the average plausibility score over all test graphs in each XAI benchmark for each of the five explainer methods.

4.2 Results

Table 2 presents the performance evaluation of the assessed explainers. The results underscore the effectiveness of the CAM explainer, which achieves the highest performance in 13 out of 15 datasets, with exceptions being *charlie* and *golf*. Specifically, Integrated Gradient demonstrates superior performance on the *charlie* dataset, while GNNEExplainer excels on the *golf* dataset.

Table 2: Plausibility results for a set of explainers on the OPENGRAPHXAI benchmarks with associated standard deviation. Best results are boldfaced.

Task		Random	Saliency	IntGrad	CAM	GNNExpl
alfa	class 0	0.524 ± 0.131	0.135 ± 0.175	0.921 ± 0.088	0.942 ± 0.068	0.673 ± 0.127
	class 1	0.481 ± 0.108	0.406 ± 0.185	0.616 ± 0.113	0.642 ± 0.144	0.450 ± 0.138
bravo	class 0	0.516 ± 0.129	0.361 ± 0.253	0.597 ± 0.137	0.697 ± 0.157	0.637 ± 0.135
	class 1	0.502 ± 0.169	0.702 ± 0.163	0.500 ± 0.017	0.988 ± 0.038	0.767 ± 0.226
charlie	class 0	0.501 ± 0.276	0.924 ± 0.148	1.000 ± 0.000	0.883 ± 0.110	0.643 ± 0.351
	class 1	0.489 ± 0.112	0.330 ± 0.144	0.406 ± 0.060	0.599 ± 0.092	0.385 ± 0.138
delta	class 0	0.485 ± 0.121	0.112 ± 0.132	0.448 ± 0.113	0.900 ± 0.113	0.494 ± 0.146
	class 1	0.492 ± 0.119	0.223 ± 0.212	0.460 ± 0.089	0.898 ± 0.079	0.520 ± 0.130
echo	class 0	0.484 ± 0.115	0.090 ± 0.145	0.726 ± 0.109	0.856 ± 0.151	0.670 ± 0.139
	class 1	0.495 ± 0.117	0.584 ± 0.184	0.526 ± 0.124	0.706 ± 0.154	0.431 ± 0.189
foxtrot	class 1	0.491 ± 0.123	0.181 ± 0.130	0.743 ± 0.099	0.930 ± 0.076	0.527 ± 0.233
golf	class 0	0.519 ± 0.156	0.039 ± 0.089	0.681 ± 0.148	0.683 ± 0.167	0.874 ± 0.180
hotel	class 0	0.431 ± 0.199	0.190 ± 0.203	0.482 ± 0.201	0.871 ± 0.247	0.486 ± 0.187
india	class 0	0.480 ± 0.159	0.245 ± 0.240	0.633 ± 0.198	0.918 ± 0.102	0.509 ± 0.190
juliett	class 0	0.464 ± 0.212	0.494 ± 0.309	0.606 ± 0.244	0.844 ± 0.226	0.540 ± 0.192
kilo	class 0	0.510 ± 0.151	0.796 ± 0.161	0.833 ± 0.073	0.947 ± 0.098	0.570 ± 0.238
lima	class 0	0.502 ± 0.136	0.123 ± 0.097	0.764 ± 0.088	0.955 ± 0.051	0.575 ± 0.254
mike	class 0	0.497 ± 0.154	0.138 ± 0.182	0.678 ± 0.167	0.840 ± 0.184	0.332 ± 0.178
november	class 0	0.531 ± 0.173	0.018 ± 0.041	0.603 ± 0.049	1.000 ± 0.004	0.408 ± 0.170
oscar	class 0	0.490 ± 0.137	0.183 ± 0.207	0.938 ± 0.082	0.973 ± 0.053	0.501 ± 0.180

A qualitative assessment of the computed explanations can be conducted by examining Figure 3, where the GT mask of a *juliett* dataset sample is compared to the explanations provided by all explainers. In this instance, the CAM explanation mask exhibits a visually superior alignment compared to the others. The strong performance of the CAM method can be attributed to its model-specific nature, as its importance scores are directly derived from the activations of the model’s units. A second example is shown in supplemental Figure 6.

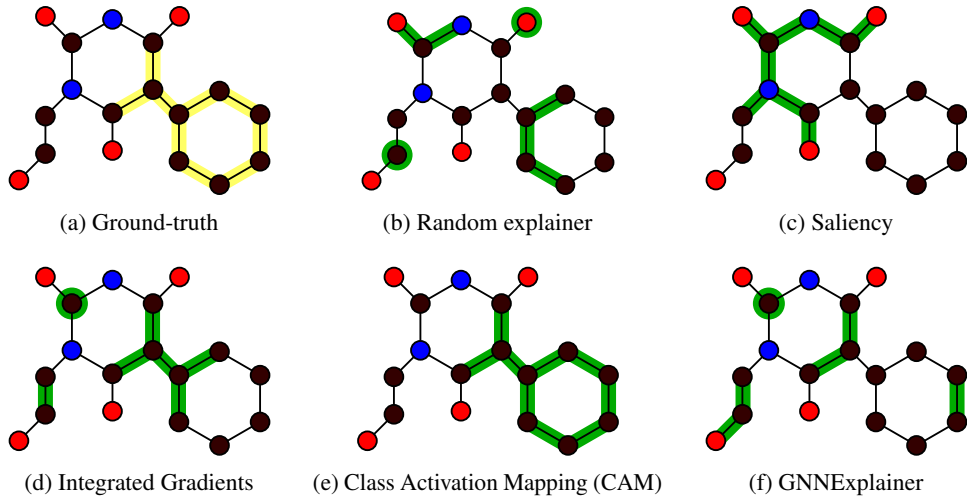


Figure 3: Explanation masks computed by the tested explainers on a test graph from the *mike* dataset. Only the top 9 nodes (GT dimension) are highlighted for each mask.

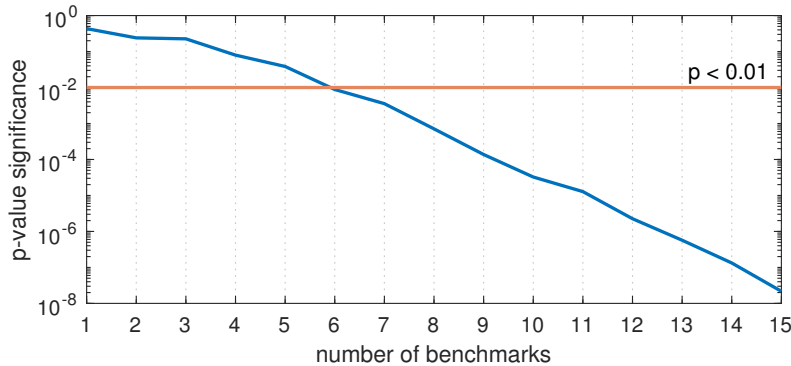


Figure 4: Statistical significance of the explainer ranking as p -value of the Friedman test (Demšar, 2006), varying the number of benchmarks considered. At least 7 benchmarks are required for $p < 0.01$ significant results. OPENGRAPHXAI benchmarks allow $p \approx 10^{-8}$, or $> 5\sigma$ significance.

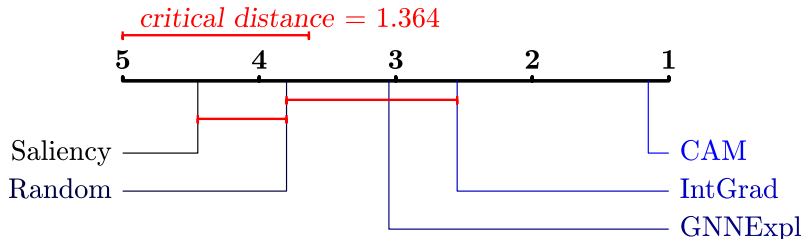


Figure 5: CAM ranks as the best explainer with significance level $\alpha = 0.05$ according to the *post-hoc* Nemenyi test (Demšar, 2006). Statistically compatible average rankings are joined in cliques.

Statistical significance To test the significance of the ranking of the explainer methods in our experiments, we apply the Friedman test (Demšar, 2006). The null hypothesis that the XAI methods’ ranking is random is rejected with $p < 10^{-7}$, or a confidence level $> 5\sigma$, in other terms. In Figure 4 we report the p -value that the Friedman test would have returned if less than the full 15 OPENGRAPHXAI had been considered in the experimental evaluation. As at least 7 benchmarks are required for $p < 0.01$ significant results, our contribution of a large collection of benchmarks is fundamental to enable researchers to drive a meaningful experimental evaluation of graph XAI methods, a task hitherto unachievable due to the benchmark scarcity.

In Figure 5 we report the critical difference diagram for the *post-hoc* Nemenyi test with significance level $\alpha = 0.05$. This test allows us to compare the ranking of graph explainers in terms of plausibility: the performance of two explainers is significantly different if the corresponding average ranks differ by at least the critical difference (Demšar, 2006). The top-ranked explainer method is CAM, which is also the statistically significant best explainer. IntGrad and GNNExpl rank below CAM beyond the critical distance, and together with Saliency, are compatible with the Random explainer.

5 Conclusions

We have introduced a method, based on the WL coloring algorithm, to automate the generation of graph XAI benchmarks from existing graph classification datasets. We apply this methodology to build a new benchmark collection, called OPENGRAPHXAI, that consists of 15 graph XAI tasks derived from 11 real-world molecular datasets. This collection provides a suite of XAI tasks to challenge the ability of graph explainers to identify the ground truths (GTs) based on structural patterns of different complexity that appear in real-world graphs. Our contribution strikes a balance between the chronic scarcity of graph XAI datasets with GTs that are annotated by domain experts, and the simplistic nature of current synthetic datasets, which are based on random graphs augmented with trivial, non-realistic motifs. To illustrate a use case, we perform an experimental evaluation of widely adopted XAI methods for graph classification. The statistical significance analysis makes it

evident the necessity of a large collection of benchmarks to draw rigorous insights to advance the progress in XAI research.

We make the code freely available at <https://github.com/OpenGraphXAI/benchmarks>, and we release the benchmarks of our collection in plain JSON format on <https://www.kaggle.com/datasets/dtortorella/ogx-benchmarks>. We also provide information to extend OPEN-GRAPHXAI collection to up to 2000+ more datasets with integrated GTs.

Limitations As stated in Section 3, our method for the construction of XAI benchmarks is restricted to GT motifs that can be distinguished via WL coloring, which in turn can be applied only to graphs with discrete input features. This restriction is necessary to avoid the combinatorial explosion of enumerating all possible sub-graphs and the computational complexity of the general sub-graph isomorphism problem. While our method can be straightforwardly extended to generate multi-class tasks, we restrict it to binary classes, which is the typical setting of previous real-world XAI benchmarks. We also generate at most a single GT motif per class, a limitation we plan to address in the future by considering general predicates on WL colors as GT explanations.

Acknowledgments and Disclosure of Funding

Research supported by: PNRR, PE00000013, “FAIR - Future Artificial Intelligence Research”, Spoke 1, funded by European Commission under NextGeneration EU programme; Project DEEP-GRAFPH, funded by the Italian Ministry of University and Research, PRIN 2022 (project code: 2022YLRBTT, CUP: I53C24002440006); Project PAN-HUB, funded by the Italian Ministry of Health (POS 2014–2020, project ID: T4-AN-07, CUP: I53C22001300001).

References

Chirag Agarwal, Owen Queen, Himabindu Lakkaraju, and Marinka Zitnik. Evaluating explainability for graph neural networks. *Scientific Data*, 10(1):144, 2023.

Roohallah Alizadehsani, Solomon Sunday Oyelere, Sadiq Hussain, Senthil Kumar Jagatheesaperumal, Rene Ripardo Calixto, Mohamed Rahouti, Mohamad Roshanzamir, and Victor Hugo C. De Albuquerque. Explainable artificial intelligence for drug discovery and development: A comprehensive survey. *IEEE Access*, 12:35796–35812, 2024. doi: 10.1109/ACCESS.2024.3373195.

Kenza Amara, Zhitao Ying, Zitao Zhang, Zhichao Han, Yang Zhao, Yinan Shan, Ulrik Brandes, Sebastian Schemm, and Ce Zhang. GraphFramEx: Towards systematic evaluation of explainability methods for graph neural networks. In Bastian Rieck and Razvan Pascanu, editors, *Proceedings of the First Learning on Graphs Conference*, volume 198 of *Proceedings of Machine Learning Research*, pages 44:1–44:23. PMLR, 09–12 Dec 2022.

Davide Baciucca, Federico Errica, Alessio Micheli, and Marco Podda. A gentle introduction to deep learning for graphs. *Neural Networks*, 129:203–221, 2020. doi: 10.1016/j.neunet.2020.06.006.

Federico Baldassarre and Hossein Azizpour. Explainability techniques for graph convolutional networks. In *ICML 2019 Workshop “Learning and Reasoning with Graph-Structured Representations”*, 2019. URL <https://arxiv.org/abs/1905.13686>.

Janez Demšar. Statistical comparisons of classifiers over multiple data sets. *Journal of Machine Learning Research*, 7:1–30, 2006.

Jia Deng, Wei Dong, Richard Socher, Li-Jia Li, Kai Li, and Li Fei-Fei. Imagenet: A large-scale hierarchical image database. In *2009 IEEE Conference on Computer Vision and Pattern Recognition*, pages 248–255, 2009. doi: 10.1109/CVPR.2009.5206848.

Giuseppe Alessio D’Inverno, Monica Bianchini, Maria Lucia Sampoli, and Franco Scarselli. On the approximation capability of GNNs in node classification/regression tasks. *Soft Computing*, 28 (13–14):8527–8547, 2024. doi: 10.1007/s00500-024-09676-1.

Mohammed Elseidy, Ehab Abdelhamid, Spiros Skiadopoulos, and Panos Kalnis. GRAMI: Frequent subgraph and pattern mining in a single large graph. *Proceedings of the VLDB Endowment*, 7(7): 517–528, 2014. doi: 10.14778/2732286.2732289.

Lukas Faber, Amin K. Moghaddam, and Roger Wattenhofer. When comparing to ground truth is wrong: On evaluating gnn explanation methods. In *Proceedings of the 27th ACM SIGKDD conference on knowledge discovery & data mining*, pages 332–341, 2021.

Matthias Fey and Jan E. Lenssen. Fast graph representation learning with PyTorch Geometric. In *ICLR Workshop on Representation Learning on Graphs and Manifolds*, 2019. URL <https://arxiv.org/abs/1903.02428>.

Michele Fontanesi, Alessio Micheli, and Marco Podda. XAI and bias of deep graph networks. In *Proceedings of the 32nd European Symposium on Artificial Neural Networks, Computational Intelligence and Machine Learning Intelligence (ESANN 2024)*, ESANN 2024, pages 41–46. Ciaco - i6doc.com, 2024. doi: 10.14428/esann/2024.es2024-85.

Bryce Goodman and Seth Flaxman. EU regulations on algorithmic decision-making and a “right to explanation”. In *ICML workshop on human interpretability in machine learning (WHI 2016)*. New York, NY, 2016. URL <http://arxiv.org/abs/1606.08813>.

Jaykumar Kakkad, Jaspal Jannu, Kartik Sharma, Charu Aggarwal, and Sourav Medya. A survey on explainability of graph neural networks, 2023. URL <https://arxiv.org/abs/2306.01958>.

Jeroen Kazius, Ross McGuire, and Roberta Bursi. Derivation and validation of toxicophores for mutagenicity prediction. *Journal of Medicinal Chemistry*, 48(1):312–320, 2005. doi: 10.1021/jm040835a.

Diederik P Kingma and Jimmy Ba. Adam: A method for stochastic optimization. In *Proceedings of the 3rd International Conference on Learning Representations*, 2015.

Nils Morten Kriege. Weisfeiler and leman go walking: Random walk kernels revisited. In Alice H. Oh, Alekh Agarwal, Danielle Belgrave, and Kyunghyun Cho, editors, *Advances in Neural Information Processing Systems*, 2022. URL <https://openreview.net/forum?id=Inj9ed0mzQb>.

Antonio Longa, Steve Azzolin, Gabriele Santin, Giulia Cencetti, Pietro Liò, Bruno Lepri, and Andrea Passerini. Explaining the explainers in graph neural networks: a comparative study. *ACM Computing Surveys*, 57(5):1–37, 2025. doi: 10.1145/3696444.

Dongsheng Luo, Wei Cheng, Dongkuan Xu, Wenchao Yu, Bo Zong, Haifeng Chen, and Xiang Zhang. Parameterized explainer for graph neural network. In H. Larochelle, M. Ranzato, R. Hadsell, M.F. Balcan, and H. Lin, editors, *Advances in Neural Information Processing Systems*, volume 33, pages 19620–19631. Curran Associates, Inc., 2020.

Alessio Micheli. Neural network for graphs: A contextual constructive approach. *IEEE Transactions on Neural Networks*, 20(3):498–511, 2009. doi: 10.1109/TNN.2008.2010350.

Christopher Morris, Nils M. Kriege, Franka Bause, Kristian Kersting, Petra Mutzel, and Marion Neumann. TUDataset: A collection of benchmark datasets for learning with graphs. In *ICML 2020 Workshop on Graph Representation Learning and Beyond (GRL+ 2020)*, 2020. URL www.graphlearning.io.

Christopher Morris, Yaron Lipman, Haggai Maron, Bastian Rieck, Nils M Kriege, Martin Grohe, Matthias Fey, and Karsten Borgwardt. Weisfeiler and Leman go Machine Learning: The Story so far. *Journal of Machine Learning Research*, 24(333):1–59, 2023.

Luca Oneto, Nicolo Navarin, Battista Biggio, Federico Errica, Alessio Micheli, Franco Scarselli, Monica Bianchini, Luca Demetrio, Pietro Bongini, Armando Tacchella, et al. Towards learning trustworthily, automatically, and with guarantees on graphs: An overview. *Neurocomputing*, 493: 217–243, 2022.

C Packer and L Holder. GraphZip: Mining graph streams using dictionary-based compression. In *Proceedings of 13th International Workshop on Mining and Learning with Graphs*, 2017.

Phillip E. Pope, Soheil Kolouri, Mohammad Rostami, Charles E. Martin, and Heiko Hoffmann. Explainability methods for graph convolutional neural networks. In *2019 IEEE/CVF Conference on Computer Vision and Pattern Recognition (CVPR)*, pages 10764–10773, 2019. doi: 10.1109/CVPR.2019.01103.

Mandeep Rathee, Thorben Funke, Avishek Anand, and Megha Khosla. BAGEL: A benchmark for assessing graph neural network explanations, 2022. URL <https://arxiv.org/abs/2206.13983>.

Kaspar Riesen and Horst Bunke. IAM graph database repository for graph based pattern recognition and machine learning. In Niels da Vitoria Lobo, Takis Kasparis, Fabio Roli, James T. Kwok, Michael Georgiopoulos, Georgios C. Anagnostopoulos, and Marco Loog, editors, *Structural, Syntactic, and Statistical Pattern Recognition*, pages 287–297, Berlin, Heidelberg, 2008. Springer Berlin Heidelberg. ISBN 978-3-540-89689-0.

Benjamin Sanchez-Lengeling, Jennifer Wei, Brian Lee, Emily Reif, Peter Wang, Wesley Qian, Kevin McCloskey, Lucy Colwell, and Alexander Wiltschko. Evaluating attribution for graph neural networks. In H. Larochelle, M. Ranzato, R. Hadsell, M.F. Balcan, and H. Lin, editors, *Advances in Neural Information Processing Systems*, volume 33, pages 5898–5910. Curran Associates, Inc., 2020.

Franco Scarselli, Marco Gori, Ah Chung Tsoi, Markus Hagenbuchner, and Gabriele Monfardini. The graph neural network model. *IEEE Transactions on Neural Networks*, 20(1):61–80, 2009. doi: 10.1109/TNN.2008.2005605.

Karen Simonyan, Andrea Vedaldi, and Andrew Zisserman. Deep inside convolutional networks: Visualising image classification models and saliency maps. In *Workshop at the 2nd International Conference on Learning Representations*, 2014. URL <https://openreview.net/forum?id=c04ycnpqxKcS9>.

Teague Sterling and John J. Irwin. Zinc 15 – ligand discovery for everyone. *Journal of Chemical Information and Modeling*, 55(11):2324–2337, 2015. doi: 10.1021/acs.jcim.5b00559.

Mukund Sundararajan, Ankur Taly, and Qiqi Yan. Axiomatic attribution for deep networks. In Doina Precup and Yee Whye Teh, editors, *Proceedings of the 34th International Conference on Machine Learning*, volume 70 of *Proceedings of Machine Learning Research*, pages 3319–3328. PMLR, 06–11 Aug 2017.

J. R. Ullmann. An algorithm for subgraph isomorphism. *Journal of the ACM*, 23(1):31–42, January 1976. doi: 10.1145/321921.321925.

Anna Varbella, Kenza Amara, Blazhe Gjorgiev, Mennatallah El-Assady, and Giovanni Sansavini. Powergraph: A power grid benchmark dataset for graph neural networks. *Advances in Neural Information Processing Systems*, 37:110784–110804, 2024.

Alex Wang, Amanpreet Singh, Julian Michael, Felix Hill, Omer Levy, and Samuel Bowman. GLUE: A multi-task benchmark and analysis platform for natural language understanding. In Tal Linzen, Grzegorz Chrupała, and Afra Alishahi, editors, *Proceedings of the 2018 EMNLP Workshop BlackboxNLP: Analyzing and Interpreting Neural Networks for NLP*, pages 353–355, Brussels, Belgium, November 2018. Association for Computational Linguistics. doi: 10.18653/v1/W18-5446.

B. Yu. Weisfeiler and A. A. Leman. A reduction of a graph to a canonical form and an algebra arising during this reduction. *Nauchno-Technicheskaya Informatsia*, 2(9):12–16, 1968.

Xifeng Yan and Jiawei Han. gSpan: Graph-based substructure pattern mining. In *Proceedings of the 2002 IEEE International Conference on Data Mining*, pages 721–724. IEEE Comput. Soc, 2002. ISBN 0-7695-1754-4. doi: 10.1109/ICDM.2002.1184038.

K. Xu, W. Hu, J. Leskovec, and S. Jegelka. How powerful are graph neural networks? In *Proceedings of the 7th International Conference on Learning Representations*, 2019.

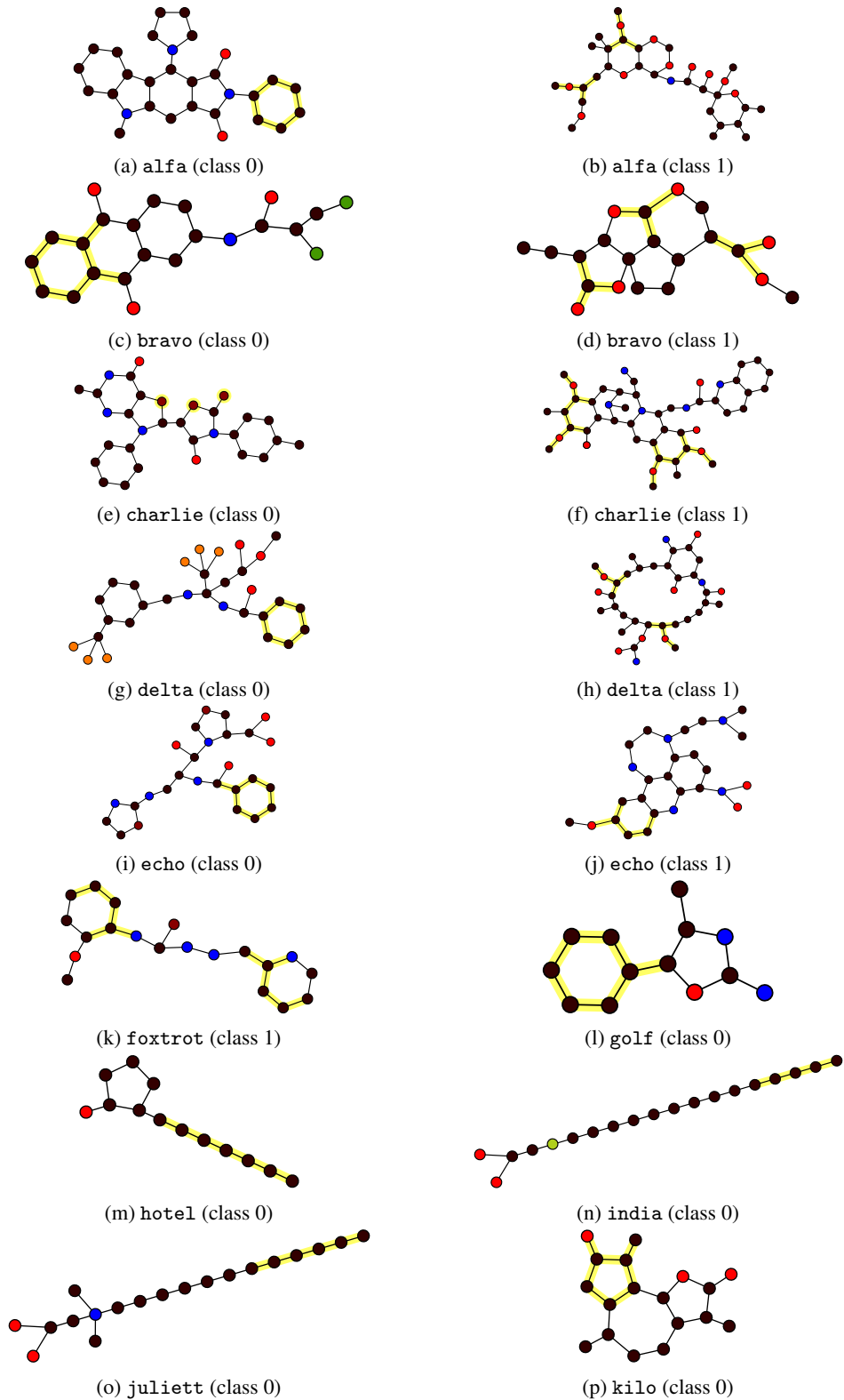
Xifeng Yan, Hong Cheng, Jiawei Han, and Philip S. Yu. Mining significant graph patterns by leap search. In *Proceedings of the 2008 ACM SIGMOD International Conference on Management of Data*, pages 433–444, New York, NY, USA, jun 2008. ACM. ISBN 9781605581026. doi: 10.1145/1376616.1376662.

Zhitao Ying, Dylan Bourgeois, Jiaxuan You, Marinka Zitnik, and Jure Leskovec. GNNExplainer: Generating explanations for graph neural networks. In H. Wallach, H. Larochelle, A. Beygelzimer, F. d'Alché-Buc, E. Fox, and R. Garnett, editors, *Advances in Neural Information Processing Systems*, volume 32. Curran Associates, Inc., 2019.

H. Yuan, H. Yu, S. Gui, and S. Ji. Explainability in graph neural networks: A taxonomic survey. *IEEE Transactions on Pattern Analysis and Machine Intelligence*, 45(05):5782–5799, may 2023. ISSN 1939-3539. doi: 10.1109/TPAMI.2022.3204236.

Bolei Zhou, Aditya Khosla, Agata Lapedriza, Aude Oliva, and Antonio Torralba. Learning deep features for discriminative localization. In *Proceedings of the IEEE conference on computer vision and pattern recognition*, pages 2921–2929, 2016.

A Ground-truths of the OPENGRAPHXAI benchmarks



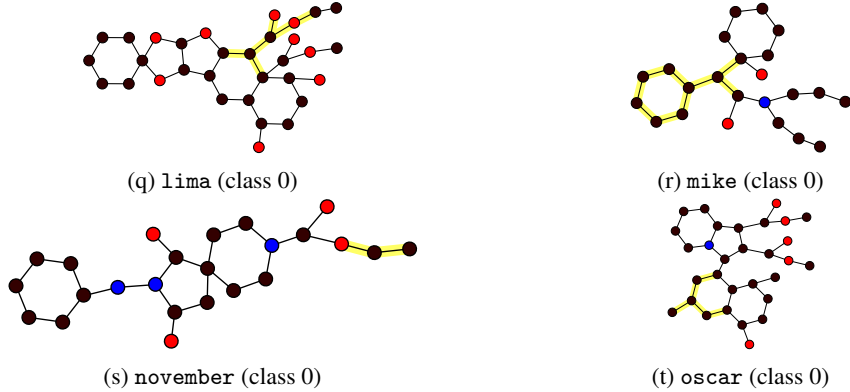


Figure 5: Examples from the datasets in OPENGRAPHXAI. GT explanations are shown with a yellow highlight.

B Experimental details

For each dataset, we train a GIN-based architecture (Xu et al., 2019) by following a hold-out model selection procedure and a grid search algorithm to optimize hyperparameters. Specifically, we split each dataset into 70% training, 20% validation, and 10% test sets. The learning rate is tuned from $\{0.001, 0.0001\}$, the number of message passing iterations (corresponding to the number of architectural layers) from $\{1, 2, 3, 4, 5\}$, the number of units for each layer from $\{32, 64\}$ and the weight decay factor from $\{0.001, 0.0001\}$. Utilizing the Adam optimizer (Kingma and Ba, 2015), models are trained for a maximum of 1500 epochs, with an early stopping patience of 30 to prevent overfitting. Model selection is based on the F1 score, and all selected models achieve a minimum of a 0.92 F1 score on the validation set. Finally, XAI techniques are employed to explain the predictions of the selected models on the test sets, and their performance is assessed by evaluating the alignment of explanations with GTs. Explainers characterized by hyperparameters have been applied with the default settings available from Fey and Lenssen (2019). All experiments have been conducted on a machine with 2 Xeon Gold 6238R of 28 cores and a base clock of 2.20 GHz each, 256 GB of RAM, and 2 GPU NVIDIA A30 featuring 3584 CUDA cores.

Table 3: Hyperparameters and performance of the selected GNN models for each task.

Task	Learning Rate	Number of Layers	Embedding Dimensions	Weight Decay	train F1	validation F1	test F1
alfa	0.0001	3	64	0.0001	0.969	0.975	0.983
bravo	0.001	4	64	0.0001	0.998	0.991	0.991
charlie	0.001	1	32	0.0001	1.000	1.000	1.000
delta	0.001	4	32	0.001	1.000	1.000	0.973
echo	0.001	4	32	0.0001	0.958	0.952	0.919
foxtrot	0.001	5	64	0.001	0.982	0.922	0.936
golf	0.001	5	64	0.0001	0.974	0.927	0.926
hotel	0.001	5	64	0.0001	0.995	1.000	0.989
india	0.001	4	32	0.001	0.992	0.975	0.983
juliett	0.001	5	32	0.001	0.966	0.989	0.989
kilo	0.001	4	32	0.001	0.999	0.995	1.000
lima	0.001	4	64	0.001	0.996	0.994	0.998
mike	0.001	5	64	0.001	0.982	0.959	0.955
november	0.001	4	64	0.001	0.999	1.000	1.000
oscar	0.001	5	32	0.0001	0.999	0.999	0.998

C Additional explanation examples

In Figure 6, we present an additional example of explanations computed by the explainers evaluated in our experiments.

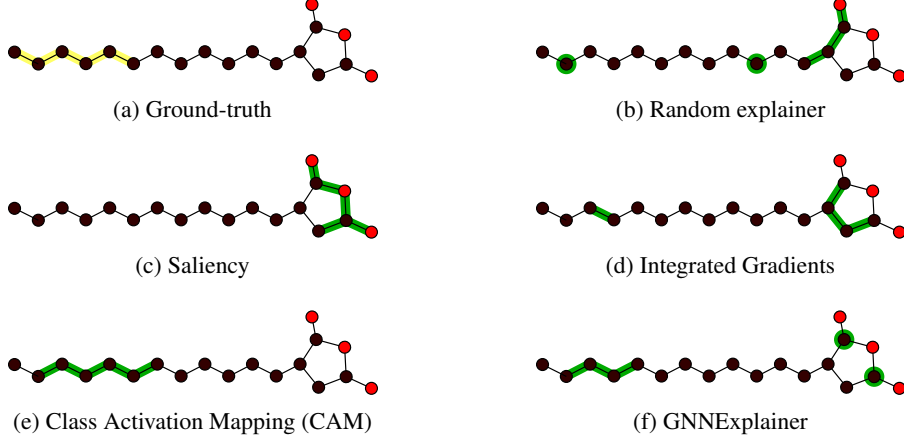


Figure 6: Explanation masks computed by the tested explainers on a test graph of the juliett dataset. Only the top 6 nodes (GT dimension) are highlighted for each mask.

D Additional background

D.1 Graph neural networks

GNNs are a class of Neural Networks able to solve tasks defined over graph-structured data. In this context, graphs are tuples $\mathcal{G}(\mathcal{V}, \mathcal{E})$ where $\mathcal{V} = \{v_i \mid i \in 1, \dots, |\mathcal{V}|\}$ is the set of nodes and $\mathcal{E} = \{(u, v) \mid u, v \in \mathcal{V}\}$ is the set of edges linking nodes. Moreover, each node is associated with local information encoded as a feature vector $\{\mathbf{x}_v \in \mathbb{R}^d \mid v \in \mathcal{V}, d \in \mathbb{N}\}$. GNNs, trained for graph classification, are parametric functions f_θ optimized to learn from data a mapping between an input graph \mathcal{G} and its associated target label $y_{\mathcal{G}}$. GNN’s computational paradigm follows a common iterative procedure known as message passing (MP). In particular, MP updates node embeddings $\mathbf{h}_v^{(\ell)}$ at each iteration ℓ based on the information extracted at iteration $\ell - 1$ and starting from the initial node input feature vector $\mathbf{h}^{(0)} = \mathbf{x}_v$ by adhering to the following general blueprint:

$$\mathbf{h}_v^{(\ell)} = \text{UPD} \left(\mathbf{h}^{(\ell-1)}, \text{AGG} \left(\left\{ \text{MSG}(\mathbf{h}_v^{(\ell-1)}, \mathbf{h}_u^{(\ell-1)}) : u \in \mathcal{N}_v \right\} \right) \right) \quad (3)$$

where MSG is a function that computes pairwise information given the node embeddings of a target node between v and each node in its neighborhood $\mathcal{N}_v = \{u : (u, v) \in \mathcal{E}\}$. AGG aggregates in a permutation invariant fashion the computed pairwise information associated with a target node, while UPD updates the target node embedding by combining $\mathbf{h}_v^{(\ell-1)}$ and the output of the AGG function. The particular implementation of the Message Passing procedure is the main discriminative factor between the diverse GNNs available in the literature.

In this work, we adopt the Graph Isomorphism Networks (GIN) Xu et al. (2019), a widely used and performant GNN variant for graph classification tasks. GIN is a convolutional GNN variant that maps each MP iteration to a layer of a deep architecture whose depth L is a tunable hyperparameter. Each layer implements MP as follows:

$$\mathbf{h}_v^{(\ell)} = \text{MLP}_{\theta^{(\ell-1)}} \left((1 + \epsilon^{(\ell-1)}) \mathbf{h}_v^{(\ell-1)} + \sum_{u \in \mathcal{N}_v} \mathbf{h}_u^{(\ell-1)} \right), \quad (4)$$

where ϵ is a learnable or fixed parameter, MSG returns the neighboring embedding, AGG is the sum function, and UPD is a sum function followed by a θ -parameterized multilayer perceptron (MLP). After L iterations, to address graph classification tasks, a global add pooling operation (Eq. 5) is applied to all node embeddings $\mathbf{h}_v^{(L)}$ to generate a single vectorial representation for the input graph $\mathbf{H}_{\mathcal{G}}$. The latter is subsequently used as input to the readout component of the network, which comprises: a linear transformation for each target class y_i (Eq. 6) to generate the logits, followed by

a softmax function (Eq. 7).

$$\mathbf{H}_G = \sum_{v \in \mathcal{V}_G} \mathbf{h}_v^{(L)}, \quad (5)$$

$$\text{logits}_{y_i} = \mathbf{w}_{y_i} \mathbf{H}_G, \quad (6)$$

$$\hat{\mathbf{y}}_G = \text{softmax}(\text{logits}) \quad (7)$$

The resulting architecture is trained end-to-end, optimizing the binary cross-entropy loss function as the generated datasets involve binary classification tasks.

D.2 Post-hoc XAI techniques

Local *post-hoc* explainers for GNNs are functions that, given as input a trained GNN f_θ and a single input graph \mathcal{G} , compute a mask $\hat{\mathbf{m}}_{\mathcal{G}} = e(f_\theta, \mathcal{G})$ that assigns importance scores to the nodes, edges, or node features of \mathcal{G} based on their relevance to the model prediction. To demonstrate the quality of the datasets comprised in our benchmark, we assess the performance of four different *post-hoc* explainers while comparing them with a **Random** baseline that assigns to each graph node a random importance values to generate the importance mask $\hat{\mathbf{m}}_{\mathcal{G}}$.

The **Saliency** method was initially applied to the image domain (Simonyan et al., 2014) and then adapted for GNNs in Baldassarre and Azizpour (2019) and Agarwal et al. (2023). It computes the gradient of the network output with respect to the input features and interprets their values as importance scores; the higher the score, the higher the importance of the associated node feature. Importances for each node are then computed as the sum of the importance scores of its features, as in Agarwal et al. (2023).

Integrated Gradients (IG) (Sundararajan et al., 2017) is a technique whose aim is to compute the contributions of the input features $\mathbf{x} \in \mathbb{R}^d$ to the output prediction y relatively to a baseline point \mathbf{x}' that encodes the complete absence of information. Specifically, IG computes the path integral of the gradients along the straight line from the baseline \mathbf{x}' to the input \mathbf{x} as:

$$\text{IG}_i(\mathbf{x}) = (x_i - x'_i) \times \frac{1}{m} \sum_{k=1}^m \frac{\delta f_\theta(\mathbf{x}' + \frac{k}{m} \times (\mathbf{x} - \mathbf{x}'))}{\delta x_i} \quad (8)$$

where x_i is a single input feature, m is the number of steps in the Riemann approximation of the integral, and f_θ is the model function. When applied to GNNs, instead, x_i is a single node input feature and the point along the path are computed on the matrix $\mathbf{X} \in \mathbb{R}^{|V| \times d}$ of node input features. As for the Saliency method, the node importance is computed by summing the importance scores of its features.

GNNExplainer (GNNExpl) Ying et al. (2019) is the most famous, used, and referenced explainable AI technique for GNNs. GNNExpl optimizes by backpropagation a soft mask looking for the best subgraph that maximizes the mutual information between the output of the model given the subgraph and the output of the model given the computational graph. It was initially developed for node classification tasks but later extended to graph classification.

Class Activation Mapping (CAM) (Zhou et al., 2016; Pope et al., 2019) is a model-specific technique that requires the model to adopt a global add pooling layer before its readout component. Specifically, CAM rewrites the computation of the individual logits (Eq: 5, 6) as a sum of node contributions:

$$\mathbf{w}_{y_i} \sum_{v \in V} \mathbf{h}_v^L + b_{y_i} = \sum_{v \in V} \left(\mathbf{w}_{y_i} \mathbf{h}_v^L + \frac{b_{y_i}}{|V|} \right) \quad (9)$$

In the formula, each addend in the rightmost summation constitutes the importance score of a node as it quantifies a node's contribution to the logit value associated with class y_i .